environmental microbiology

Environmental Microbiology (2021) **23**(1), 448–463 doi:10.1111/1462-2920.15331

Diversity and biomass dynamics of unicellular marine fungi during a spring phytoplankton bloom

Taylor Priest[1], **Bernhard Fuchs**[1], **Rudolf Amann**[1] **and Marlis Reich**[2*]

[1]*Department of Molecular Ecology, Max Planck Institute for Marine Microbiology, Bremen, Germany.*

[2]*Molecular Ecology Group, FB2, University of Bremen, Bremen, Germany.*

Summary

Microbial communities have important functions during spring phytoplankton blooms, regulating bloom dynamics and processing organic matter. Despite extensive research into such processes, an in-depth assessment of the fungal component is missing, especially for the smaller size fractions. We investigated the dynamics of unicellular mycoplankton during a spring phytoplankton bloom in the North Sea by 18S rRNA gene tag sequencing and a modified CARD-FISH protocol. Visualization and enumeration of dominant taxa revealed unique cell count patterns that varied considerably over short time scales. The Rozellomycota *sensu lato (s.l.)* reached a maximum of 10^5 cells L^{-1}, being comparable to freshwater counts. The abundance of Dikarya surpassed previous values by two orders of magnitude (10^5 cells L^{-1}) and the corresponding biomass (maximum of 8.9 mg C m^{-3}) was comparable to one reported for filamentous fungi with assigned ecological importance. Our results show that unicellular fungi are an abundant and, based on high cellular ribosome content and fast dynamics, active part of coastal microbial communities. The known ecology of the visualized taxa and the observed dynamics suggest the existence of different ecological niches that link primary and secondary food chains, highlighting the importance of unicellular fungi in food web structures and carbon transfer.

Introduction

The presence of fungi in marine ecosystems has long been known, but their significance largely overlooked. Only recently, through environmental sequencing surveys, has their ubiquitous distribution and high diversity been revealed (Wang *et al*., 2014; Zhang *et al*., 2015; Comeau *et al*., 2016; Taylor and Cunliffe, 2016; Duan *et al*., 2018). Such studies have provided a valuable base-line understanding of marine fungi but much more work is required before we can understand their ecological roles and contribution to biogeochemical processes. In particular, information regarding cellular abundances, biomass and dynamics of dominant taxa over short-time scales is lacking (Grossart *et al*., 2019).

Pelagic fungi (mycoplankton) in the coastal environment have been shown to represent a diverse range of taxonomic groups and are able to accumulate considerable biomass, comparable to prokaryotes (Gutiérrez *et al*., 2010). The structure of these communities appears to vary with latitude and local influences, with evidence suggesting a dominance by members of the Dikarya (Ascomycota and Basidiomycota) or the Chytridiomycota (Comeau *et al*., 2016; Hassett *et al*., 2016; Tisthammer *et al*., 2016; Duan *et al*., 2018). Time-series data have also highlighted the impact of seasons on community composition and more specifically, changes in nutrients, temperature and, with respect to certain taxa, phytoplankton (Taylor and Cunliffe, 2016; Duan *et al*., 2018; Banos *et al*., 2020). To understand these driving factors further, a few studies have tried to elucidate ecological roles for the dominant fungal taxa and revealed the presence of parasitism and saprotrophism within the water column (Gutiérrez *et al*., 2016; Scholz *et al*., 2016; Cunliffe *et al*., 2017). Cunliffe *et al*. (2017) isolated several annually recurring mycoplankton strains from the English Channel and showed their ability to degrade phytoplankton-derived polysaccharides. In the coastal Arctic environment, Hassett and Gradinger (2016) used epifluorescence microscopy to visualize fungal parasitism of diatoms in sea-ice and seawater while Ishida *et al* (2015) described a great fungal taxonomic diversity associated with single freshwater phytoplankton cells. These insights would suggest that mycoplankton are active members of coastal ecosystems and likely perform important ecological functions during phytoplankton blooms. However, until now, none of the studies provide

Received 11 June, 2020; revised 11 November, 2020; accepted 12 November, 2020. *For correspondence. Tel. +49 (0)421 218 62825; Fax: +49 (0)421 218 98 62825; E-mail reich@uni-bremen.de.

short-time scale information on mycoplankton dynamics over an entire phytoplankton bloom.

Spring phytoplankton blooms are annually recurring phenomena in temperate and polar latitudes, responsible for fixing vast quantities of CO_2 and supplying essential organic matter to the ecosystem (Falkowski *et al*., 1998; Field *et al*., 1998). This organic matter drives substantial changes in the microenvironment, providing valuable ecological niches and fuelling the respiration of heterotrophic picoplankton (Teeling *et al*., 2012; Buchan *et al*., 2014). With evidence of saprotrophism and parasitism on diatoms being reported, it could be expected that, as has been observed in a drinking water reservoir (Zhang *et al*., 2018), phytoplankton blooms would drive distinct changes within the fungal community, with differential effects across taxa reflecting their ecological niches.

To understand an organism's ecology and role within an environment, information regarding its abundance is of vital importance. Abundance data for mycoplankton are scarce and efforts to retrieve such information have been principally focused on freshwater systems with a few, more recent marine studies adopting similar techniques. The most widely used approaches involve cell wall staining with CalcoFluor White, a non-specific fluorescent dye that binds to chitin and cellulose, and the quantification of ergosterol, a sterol biomarker mostly restricted to the fungal kingdom. These methods have provided invaluable insights into fungal ecology, from determining the contribution of fungi to organic material decomposition in lakes and streams (Ravelet *et al*., 2001; Nikolcheva *et al*., 2003) to visualizing interactions with phytoplankton (Rasconi *et al*., 2009; Gutiérrez *et al*., 2016) and quantifying the biomass of larger septate hyphae in a coastal upwelling system (Gutiérrez *et al*., 2010). However, there are clear fundamental limitations, namely the inability to capture the whole fungal kingdom. It has been shown that a number of fungal lineages lack ergosterol synthesis pathways, while non-fungal protists contain such systems (Weete *et al*., 2010), and basal fungal lineages lack chitin in their cell wall in some or all of their life stages (James and Berbee, 2011). A more promising approach is FISH, which has already provided considerable advancements in our understanding of aquatic bacterial ecology over the past two decades (Pernthaler *et al*., 2002; Wagner and Haider, 2012). A small number of studies have used a targeted FISH approach to observe specific fungal taxa in aquatic systems, typically focusing on the basal lineages that lack complex cell wall structures (Jobard *et al*., 2010; Hassett *et al*., 2019), but no kingdom-wide approach is currently available.

We aim to address current knowledge gaps while analysing the dynamics of unicellular mycoplankton in the 0.2–10 μm size fraction over the entire course of a spring phytoplankton bloom at the long-term ecological research station (LTER), Helgoland Roads, Germany. An almost daily sampling regime for high-throughput sequencing was applied, revealing the short-time scale dynamics of prominent groups and acting as a reference for the design of 18S rRNA gene oligonucleotide probes. The probes were designed at a phylum and OTU-level and combined with a novel catalysed reporter deposition-fluorescence *in situ* hybridization (CARD-FISH) protocol to acquire accurate data on the morphologies and cell abundances of dominant taxa.

Results

Phytoplankton bloom and physicochemical parameters

The 2017 spring phytoplankton bloom at Helgoland Roads spanned from the 6th of April to the 17th of May, with a maximum chlorophyll *a* peak of 10 mg m^{-3} occurring on the 28th April (Fig. 1). The bloom was dominated by pennate diatoms (Fig. S1). During the sampling period, distinct changes were observed in the measured physicochemical parameters. Briefly, temperature increased from 5.2°C to 10.5°C and nutrient concentrations typically reached a maximum prior to the peak in chlorophyll *a*, before decreasing significantly (Table S1).

Mycoplankton community: structure, diversity and potential impact of environmental parameters

A total of 166 653 sequence reads were classified as fungi and clustered into 681 operational taxonomic units (OTUs), spanning 36 orders and 16 classes of five phyla. By inserting sequences phylogenetically into the fungal reference tree, it was possible to capture and classify so far undescribed taxa at different taxonomic levels. In total, two clades representing novel diversity were designated under the Ascomycota, two under the Basidiomycota, and three within the Rozellomycota *s.l*. (Fig. S2).

The most prevalent phyla, in descending order, were the Basidiomycota, Rozellomycota *s.l*., Ascomycota and Chytridiomycota. Although a large diversity was identified within these phyla, each was dominated by only a few OTUs (Fig. 1). The five most abundant OTUs in the dataset represented >70% of the reads and were identified as: OTU163 (Microbotryomycetes *s.l*. Clade 1) = 36% of reads, OTU209 (Rozellomycota *s.l*. Clade 3) = 14% of reads, OTU472 (Ascomycota *s.l*. Clade 1) = 13% of reads, OTU333 (Chytridiomycetes) = 6.1% of reads and OTU571 (Rozellomycota *s.l*. Clade 2 sub clade 1) = 4.6% of reads. The fluctuations in these OTUs

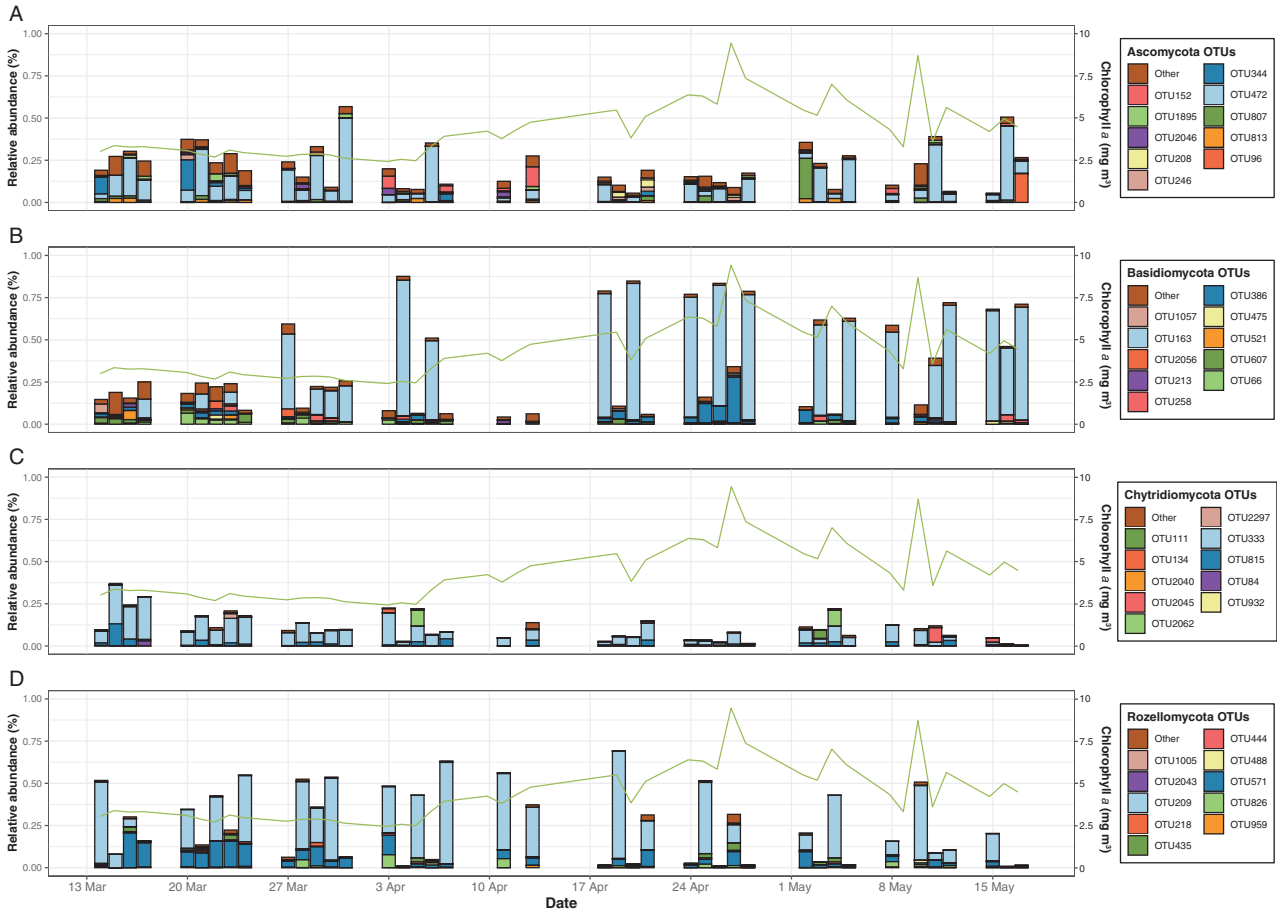

Fig 1. Relative read abundance of the dominant OTUs within each phylum (bars) along with the chlorophyll a values (line) as a proxy for the phytoplankton bloom (s.l. = sensu lato). [Color figure can be viewed at wileyonlinelibrary.com]

were largely responsible for the dynamics observed at a lower taxonomic resolution.

The community composition in the pre-bloom period was the most taxonomically rich, as indicated by Chao1 and Shannon diversity indices (Fig. S3), with considerable contributions from the Chytridiomycetes, Rozellomycota *s.l.* clade 2 and clade 3, Ascomycota *s.l.* clade 1 and Eurotiomycetes (Fig. S4). After the first week of sampling, distinct shifts were observed, most notably a decrease of Chytridiomycota and Eurotiomycetes, coinciding with an increase in Rozellomycota *s.l.* clade 3 and a less pronounced increase in Microbotryomycetes. With the on-set of the phytoplankton bloom, an alternating dominance pattern was observed between the Microbotryomycetes and lineages of the Rozellomycota *s.l.* phylum, particularly clade 3. This dynamic persisted until the decline in chlorophyll *a*, which coincided with a significant reduction in the contribution of Rozellomycota *s.l.* clades and Chytridiomycota, while Microbotryomycetes remained dominant (Fig. S4).

Assessing the influence of the measured parameters using a redundancy analysis resulted in 56% of the variation in OTU dynamics being constrained (Fig. S5). However, to more accurately determine the statistically significant parameters, a forward stepwise model building was carried out. This concluded that temperature and chlorophyll *a* combined, provided the best, statistically significant, model for understanding the observed variations of mycoplanktonic community structure, although they only captured 17% of the variation. When analysing only the most dominant OTU from each phyla, temperature was identified as the most influencing parameter, positively associated with Microbotryomycetes OTU163 while negatively associated to the Chytridiomycota OTU333 and Rozellomycota *s.l.* OTU571. Chlorophyll *a* concentration and diatom abundance also showed a positive association to OTU163 and the Ascomycota OTU472 respectively. Contrarily, the dominant Rozellomycota *s.l.* OTU209 showed no relation to any of the tested variables (Table 1).

CARD-FISH results

Applying our modified CARD-FISH protocol to 26 samples (of the 0.2–3 μm and 3–10 μm fraction) over the bloom resulted in successful, bright signals being observed for each of the designed probes. For the Ascomycota and Basidiomycota probes, the signals originated from single cell forms, typically ovoid in shape with a diameter of 2–7 μm (Fig. 2). The combination of the FBas_757 probe with CalcoFluor White staining further confirmed the cells to be of fungal origin (Fig. S6). Filamentous structures were almost entirely absent from the samples and the very few observed were not included in the analysis. The cell counts provided for the Dikarya (summed FBas_757 and FAsc_1094 counts) were derived solely from the 3–10 μm fraction, as no signals were observed in the 0.2–3 μm fraction. Enumeration of the signals in the 3–10 μm fraction revealed distinct fluctuations in abundance over the sampling period (Fig. 3A), which often differed from the tag-sequencing results. The Ascomycota were initially present in low abundance (6.9×10^3 cells L^{-1}) but exhibited two peaks, the first following the on-set of the phytoplankton bloom (3.6×10^4 cells L^{-1}) and the second occurring after the chlorophyll *a* maximum (7.4 x 10^4 cells L^{-1}). A similar pattern was observed for the Basidiomycota, although the maximum values were significantly higher. The second, and most pronounced, Basidiomycota peak reached 2.6×10^5 cells L^{-1}. The Pucciniomycotina, as expected, agreed with the Basidiomycota dynamic, except lower abundances were reached (maximum 1.1×10^5 cells L^{-1}).

With respect to the Rozellomycota *s.l.*, the two OTU-level probes both revealed ovoid cell shapes with diameters ranging from 1–3 μm. Despite this cell size range, only 15%–32% of the cell counts were derived from the 0.2–3 μm fraction (Table S2). Enumeration of signals in both fractions resulted in the same abundance patterns over the bloom and, therefore, the values were combined and analysed as one. The resulting counts revealed distinct dynamics between the two OTUs (Fig. 3A). OTU571 was at the highest abundance, 2.8×10^4 cells L^{-1}, in the first 2 weeks of sampling and reduced considerably with the on-set of the phytoplankton bloom, remaining in low but consistent abundance from thereon. In contrast OTU209 was in low abundance initially and showed a sharp increase with the on-set of the phytoplankton bloom followed by a gradual, step-like decrease, with a maximum abundance of 1.06×10^5 cells L^{-1}.

Dikarya biomass and driving environmental parameters

The per cell biovolume of Dikarya cells identified using CARD-FISH ranged from 4.19 μm^3 to 179.59 μm^3, with an average of 33.51 μm^3. The average biovolume was used to calculate the total biomass of Dikarya yeast-like cells in each sample, applying the yeast-specific conversion factor proposed by van Veen and Paul (1979) of 1 μm^3 = 0.8 pg C. The total biomass ranged from 0.37 mg C m^{-3} to 8.9 mg C m^{-3} after the chlorophyll *a* peak, almost a 30-fold increase (Fig. 3B). Statistical analyses identified temperature and silica as the most influencing factors, explaining 45% of the Dikarya biomass variation (Table 2). The same variables were the most influencing on the Basidiomycota abundance. The variation in Ascomycota was best explained by Dinoflagellate abundance, while the OTU571 was most influenced by salinity. Similarly to the relative abundance variation, the absolute abundance of OTU209 showed no significant relation to the tested variables.

Discussion

Currently, our knowledge on marine mycoplankton is largely derived from tag-sequencing data while quantitative information is scarce (Grossart *et al*., 2019). Therefore, we modified a CARD-FISH protocol using pure cultures to cover most major groups within the fungal kingdom and subsequently applied it to the 0.2–3 and 3–10 μm fraction of the fungal community during a spring phytoplankton bloom. Aquatic fungi in this size range have been well-studied in freshwater environments where they perform several ecologically important roles; these include parasitism on phytoplankton (Kagami *et al*., 2007; Sime-Ngando, 2012), acting as a valuable food source for zooplankton (Frenken *et al*., 2018) and saprotrophic degradation of pollen (Wurzbacher *et al*., 2014), leaf-litter

Table 1. Results of stepwise model building in 'both' directions with permutation tests (P < 0.05) using the normalized sequence read abundance of the top five most abundant OTUs and environmental parameters.

OTU name/taxa	Significant environmental parameters	Linear regression coefficient	Linear regression adjusted R^2 value
OTU163 (Microbotryomycetes)	Temperature + chlorophyll *a*	0.24	0.257
OTU209 (Rozellomycota *sensu lato* Clade 3)	NA	NA	NA
OTU472 (Ascomycota Clade 1)	Diatoms	0.046	0.007
OTU333 (Chytridiomycetes)	Temperature	−0.07	0.48
OTU571 (Rozellomycota *sensu lato* Clade 2)	Temperature	−0.05	0.23

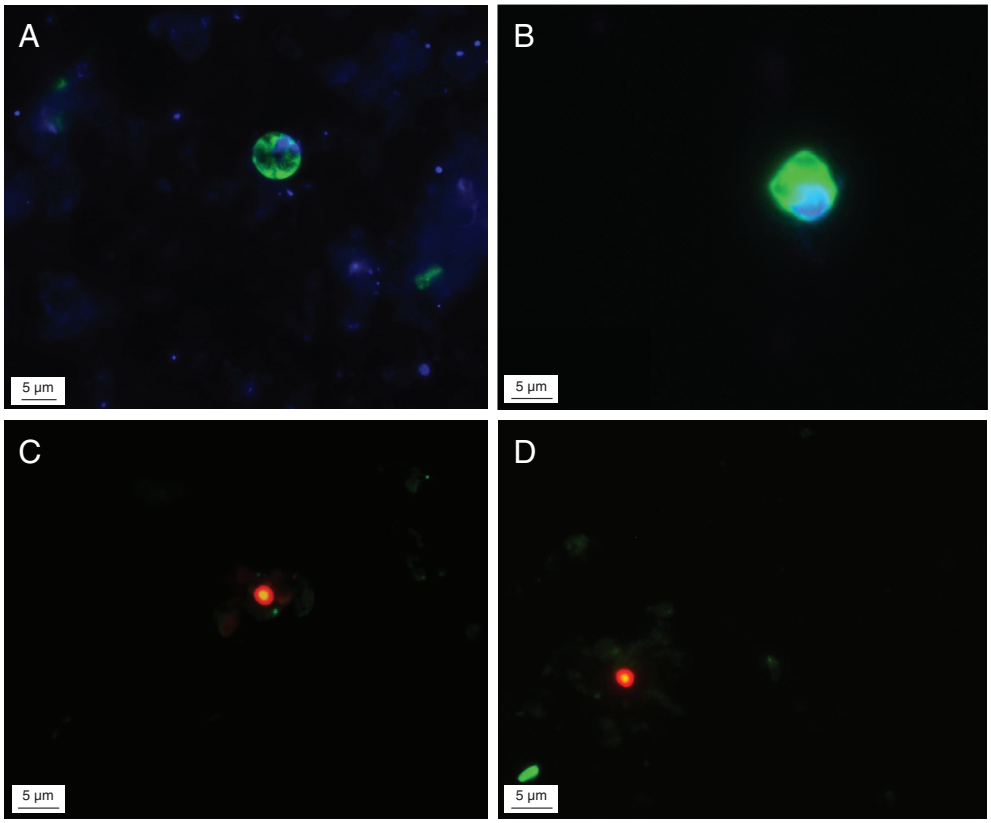

Fig 2. CARD-FISH images of typical cell morphologies identified in this study. Photos taken on a Zeiss Axio D2 Imager at 100x magnification. In images A and B: blue = DAPI and green = probe, in images C and D: orange/yellow = Sybr Green and red = probe. A. and B. Basidiomycota probe, C. OTU209 (Rozellomycota *s.l*. clade 3) probe and D. OTU571 (Rozellomycota *s.l*. clade 2) probe. [Color figure can be viewed at wileyonlinelibrary.com]

(Nikolcheva *et al*., 2003) and particulate organic matter (Wurzbacher *et al*., 2015). In contrast, they remain largely understudied in the marine environment. We combined the modified CARD-FISH protocol with an almost daily tag sequencing sampling regime resulting in (i) the identification of short-time scale dynamics of the mycoplankton community, (ii) the first taxon- and OTU-specific cell numbers (and biomass) for dominant mycoplankton and (iii) the first visualization of Rozellomycota *s.l*. in the marine environment.

The mycoplankton community was characterized by a high diversity of OTUs spanning across the fungal kingdom, branching with well-known organisms or within clusters formed solely by novel diversity. The majority of reads were assigned to the Ascomycota, Basidiomycota and Rozellomycota *s.l*. but, despite the diversity found, each phyla was dominated by only one or two OTUs. The low number of temporally dominant OTUs seems to be a general pattern of mycoplankton communities in coastal environments (Taylor and Cunliffe, 2016; Picard, 2017), where they can peak in abundance several times a year and be categorized according to such patterns (Banos *et al*., 2020). The fluctuations can be attributed to a direct or indirect effect of periodically changing environmental conditions, typical of coastal environments (Jeffries *et al*., 2016; Taylor and Cunliffe, 2016; Duan *et al*., 2018; Banos *et al*., 2020). Important factors include periodic transport of water masses with riverine inputs, tidal mixing, wind forcing and sediment resuspension (Tian *et al*., 2009). Helgoland Roads is not strictly a coastal environment but is positioned at a transition zone between coastal and off-shore waters, resulting in varying influences and a dynamic system (Hickel *et al*., 1992; Wiltshire *et al*., 2010). However, multi-year studies conducted on the spring phytoplankton bloom at Helgoland Roads have reported recurring patterns in the bacterial community that are driven by specific substrate niches (Teeling *et al*., 2016; Chafee *et al*., 2018). Similar to the bacterial community, the shift in dominance from Rozellomycota *s.l* in pre- and early- bloom stages to Basidiomycota in mid- to late-bloom stages reported here, likely also reflects their occupation of distinct ecological niches rather than direct effects of fluctuating abiotic conditions.

The Dikarya

The OTUs assigned to the Dikarya were either clustered with well-known yeast or dimorphic fungi (Kurtzman

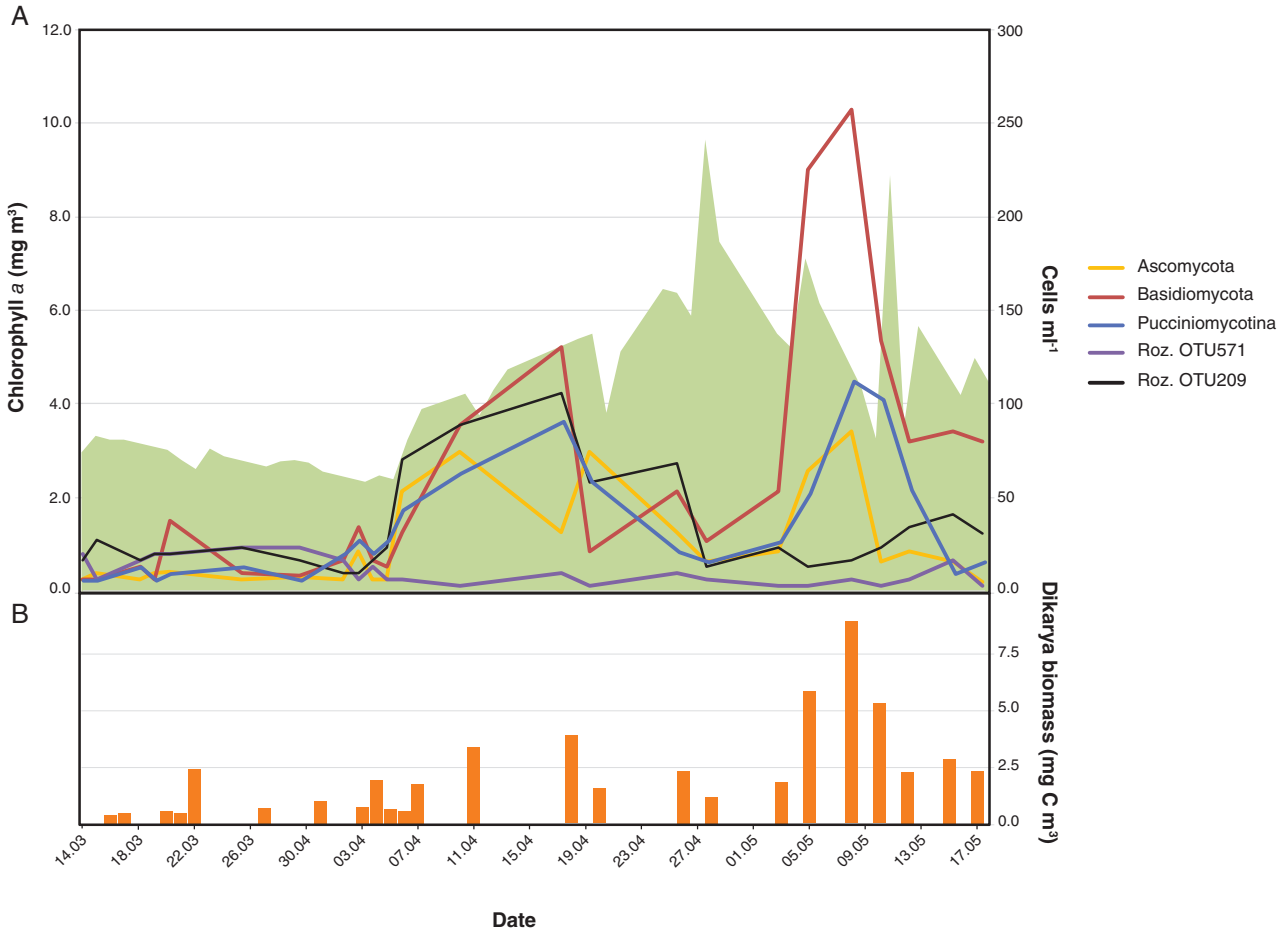

Fig 3. Fungal cell count and biomass values.
A. Absolute abundance of dominant fungal taxa enumerated using CARD-FISH (lines) with the chlorophyll *a* values as a proxy for the phytoplankton bloom (area) (Roz. = Rozellomycota).
B. Total yeast biomass calculated by applying a conversion factor on the cell count values of Ascomycota and Basidiomycota. [Color figure can be viewed at wileyonlinelibrary.com]

Table 2. Results of stepwise model building in 'both' directions with permutation tests ($P < 0.05$) using the absolute, CARD-FISH derived, cell counts and biomass values of dominant fungi OTU/taxa and measured parameters.

Name	Significant environmental parameters	Linear regression coefficient	Linear regression *adjusted* R^2 value
Ascomycota	Dinoflagellates	−0.048	0.27
Basidiomycota	Temperature	0.09	0.57
	+ silica	−0.05	
Pucciniomycotina	Nitrate	0.05	0.27
OTU571	Salinity	0.13	0.65
OTU209	NA	NA	NA
Dikarya biomass	Temperature	0.12	0.41
	+silica	-0.004	

et al., 2011) or formed novel branches on the phylogenetic tree. Within the Basidiomycota, such groups included the genera *Symmetrospora* (including the previously named *Rhodotorula* and *Sporobolomyces*(Wang *et al*., 2015; Wijayawardene *et al*., 2020)) and *Rhodosporidium,* and within the Ascomycota, the classes Saccharomycetes, Eurotiomycetes and Leotiomycetes. The dominance of yeast(-like) forms could be expected from the size fraction sampled, which could also include spores or fragmented hyphae. Application of our modified CARD-FISH protocol with phylum and sub-phylum level probes further supported this. Fluorescent signals were

observed for ovoid and ellipsoidal cell shapes with a diameter of 2–7 μm. The cell morphologies and taxonomic affiliation of dominant OTUs lead us to believe that these are yeast cells or yeast-like cell stages of dimorphic fungi. It is important to note that the presence of spores, like those from filamentous fungi, cannot be completely excluded, but sporulation in water is reduced and the release is often passive (Heitman *et al*., 2017). Furthermore, the highly dynamic cell abundance patterns combined with the bright hybridization signals observed under the microscope make us believe that the majority of the visualized cells are metabolically active.

The cell counts of yeast(-like) Dikarya reported here, 10^5 cells L^{-1}, are two orders of magnitude higher than those previously reported for coastal and heavily polluted environments using traditional light microscopy (Kutty and Philip, 2008). It is also likely that our values do not represent the annual maximum. Meyers *et al*. (1967) enumerated pelagic yeasts at Helgoland Roads over 3 years and reported seasonal variations with peak values in the third quarter of the year. The ability for the cell counts to reach such values and change dramatically over short time scales is likely owing to the division forms and cell cycles of yeasts. In laboratory cultures, doubling times as short as 100 min have been shown for budding yeasts (Slater *et al*., 1977). However, Mitchison-Field *et al*. (2019) recently identified new division forms in marine isolates, such as spherical division, multiple budding or readily transitioning between both in a single generation, allowing for a single mother cell to generate several daughter cells at once. These findings highlight our currently limited knowledge on marine yeast ecology and the need for modern microscopy-based techniques, such as the CARD-FISH protocol presented here, to be incorporated into environmental surveys.

In order to compare our findings with more recent studies and provide additional ecological data, we converted our cell counts to biomass. The total Dikarya biomass reached a maximum of 8.9 mg C m^{-3} following the chlorophyll *a* peak, with an average of 2.2 mg C m^{-3}. In Arctic coastal seawater, the average fungal biomass has been reported as 1.02 mg C m^{-3} by Hassett *et al*. (2019) using an ergosterol-based method. However, due to those values representing all planktonic size-fractions, the total biomass of the unicellular Dikarya is likely much lower. Generally, the lower biomass reported in the Arctic samples is expected, reflecting the lower productivity of this ecosystem in comparison to a temperate site in spring. In comparison, Gutiérrez *et al*. (2010) quantified the biomass of septate hyphae in a three-year monitoring programme in the Chilean upwelling system using CalcoFluor-White staining and epifluorescence microscopy. They reported significant seasonal variations in carbon biomass with peak values coinciding with high phytoplankton productivity, but typically the values rarely exceeded 10 mg C m^{-3}; similar to the maximum values reported here (8.9 mg C m^{-3}). This is surprising, due to the nutrient rich system sampled by Gutiérrez *et al*. (2010) and their focus on fungal structures that, due to their morphology, already have a significantly higher biomass than unicellular fungi. We have to note that due to limited data on yeast biovolume to biomass conversion, the biomass calculated here may be a slight over- or under-representation. Despite this, the rapid change in abundance and biomass over such short time scales indicates that yeast(-like) Dikarya are actively playing a role during spring phytoplankton blooms.

Yeasts are known to be metabolically versatile and have the capacity to use a wide range of carbon sources, although they preferentially metabolize carbohydrates (Gancedo, 1986). This versatility is reflected in the distribution of aquatic yeasts, which have been isolated from solid substrates such as particulate organic matter (POM) (Wurzbacher *et al*., 2014, 2015) and macroalgae (Loque *et al*., 2010; Francis *et al*., 2016), and associated with polycyclic aromatic hydrocarbon transformation (MacGillivray and Shiaris, 1993) and changes in dissolved organic matter (DOM) concentrations (Jørgensen and Stepanauskas, 2009; Wurzbacher *et al*., 2014). Their distribution has also been suggested to reflect the trophic condition of the environment, with cell densities increasing with pollution and algal blooms (Hagler and Mendonça-Hagler, 1981; Hagler, 2006). Reported associations with algae and algal-derived organic matter would suggest that, like their terrestrial counterparts, they are performing saprotrophic roles. Cunliffe *et al*. (2017) provided initial evidence supporting this, showing assimilation of algal-derived particulate organic carbon by a basidiomycetous yeast during labelled-substrate experiments. The shear diversity in composition and structure of released organic matter during a phytoplankton bloom (Suksomjit *et al*., 2009; Thornton, 2014) could provide a substantial source of nutrients for yeasts and is likely the driving factor behind the dynamics observed in this study. Whether the preferred substrates are of particulate or dissolved origin is yet unclear. Microscopy observations in this study showed evidence of 'particle-associated' and 'free-living' single-cell Dikarya. Ecologically speaking, attaching to solid substrates such as particles provides numerous advantages in a dilute medium like seawater, as it acts as a nutrient hotspot and prevents loss of substrate and enzymes during osmotrophic growth. However, their ability to use a broad set of carbon sources, from alcohols and amino acids to hexose sugars and two-carbon compounds (Rosa and Péter, 2006), may allow them to occupy broad niches of dissolved substrates during phytoplankton blooms. Most likely, they do not strictly use DOM or POM but a combination of both. It

could be anticipated that pelagic yeasts are capable of steady growth from the diverse DOM substrate pool but can grow and reproduce faster when adsorbed to POM particles.

The observed growth dynamics of Basidiomycetous yeasts in this study, an 11-fold increase over 1 week, surpasses what has previously been recorded for the most responsive bacterial taxa: a fivefold increase in 1 week (Teeling *et al*., 2012). This magnitude of growth would suggest that, like responsive bacterial taxa during phytoplankton blooms, these yeasts represent opportunistic r-strategists, responding rapidly to the availability of metabolizable substrates. Therefore, as has been previously suggested, we believe that yeast(-like) Dikarya contribute to the degradation of organic material released during a phytoplankton bloom and are thus capable of fueling the mycoflux (Grossart *et al*., 2019).

The Rozellomycota sensu lato

The Rozellomycota are an understudied phylum that forms one of the earliest diverging fungal lineages (Tedersoo *et al*., 2018). Their phylogenetic positioning has been determined mostly from environmental sequences (Lara *et al*., 2010; Jones *et al*., 2011), leading to much debate about their affiliation to other fungal taxa and closely related organisms (James *et al*., 2013; Letcher and Powell, 2018; Wijayawardene *et al*., 2020). Microscopy-based studies have revealed a multistage life cycle consisting of an obligatory parasitic stage and a motile zoosporic stage, which lacks chitin in the cell wall (James and Berbee, 2011; Jones *et al*., 2011). Proteomic and genomic features of Rozellomycota also indicate a parasitic lifestyle, with the absence of many primary metabolism genes, such as those involved in *de novo* nucleotide synthesis, suggesting host-dependency (James *et al*., 2013; Torruella *et al*., 2018). Until now, only one genus and less than 30 species have been described (Letcher and Powell, 2018). Therefore, it is no surprise that the high number of OTUs reported here formed several new clusters within the phylogenetic tree. This high novel diversity has so far hindered accurate detection in environmental sequencing surveys, culminating in contradictory distribution data. In pelagic marine systems, the Rozellomycota are typically reported to be present in low but stable abundances (Livermore and Mattes, 2013). However, a study conducted across large regions of the Baltic Sea suggested that at some sampling sites, they were the dominant taxa within the mycoplankton community (Rojas-Jimenez *et al*., 2019). This latter find reflects the patterns observed in lacustrine ecosystems (Rojas-Jimenez *et al*., 2017) where, in some cases, they can be the most prominent protistan group (Taib *et al*., 2013). The high diversity identified in our dataset, is in agreement with the data from the TARA ocean expedition that revealed a relatively large and diverse pool of free-living parasites in the eukaryotic pico-nanoplankton of the photic zone (de Vargas *et al*., 2015). The rich diversity of such organisms was suggested to reflect the myriad abundant hosts. Similarly, the high diversity of OTUs assigned to Rozellomycota *s.l*. identified here, likely reflects the broad host range of this phylum. Previous studies have reported smaller phytoplankton taxa, stramenopiles and other fungal taxa as hosts. Thus, they are secondary consumers in both producer and detritus based food webs, which may have marked effects on food web dynamics (Gleason *et al*., 2012).

To further investigate the dynamics of the dominant members of the Rozellomycota *s.l*., we designed highly specific probes for the two most prominent OTUs. The successful visualization of ovoid cells using the OTU-specific probes represents, to our knowledge, the first microscopy evidence of this phylum in the marine environment. Jones *et al*. (2011) had previously detected Rozellomycota in freshwater samples, but application of the same probes to marine samples resulted in no signals. We assume this was due to the high specificity of the probes used, as they covered only a fraction of the phylum, as represented in our database. With the probes developed here, we report maximum cell numbers of 10^5 cells L^{-1}, constituting up to 46% of total fungal cell counts with CARD-FISH. The observed cell shapes and sizes (1–3 μm) are in accordance with those previously described for freshwater motile zoospores, while resting spores are typically larger (>10 μm) (James and Berbee, 2011) and thus are not in the size-fraction sampled here. Despite this cell size, the majority of cells were found on the 3–10 μm fraction. However, this is likely an artefact of filtration and influenced by the high concentration of organic material on the filters. It is important to note that the specificity of our approach likely underrepresents the actual number of Rozellomycota *s.l*. in the samples, as we targeted solely the two most abundant OTUs. In comparison, cell abundances in freshwater environments have been reported at values up to 10^6 cells L^{-1}. In such systems, zoosporic fungi, like Chytridiomycota and Rozellomycota, are an important component of food web structures (Gleason *et al*., 2012; Sime-Ngando, 2012; Voigt *et al*., 2013). They infect large, grazing-resistant phytoplankton species and use the host's nutrients and organic material to form new zoospores, which can be grazed by zooplankton. Thus, zoospores provide an important trophic link between phytoplankton and zooplankton, termed 'mycoloop', which may shape aquatic systems by altering food web dynamics and sinking fluxes (Kagami *et al*., 2014). Since our zoospore counts provide comparable values that are

considered to be ecologically significant for the freshwater mycoloop, it can be assumed that marine Rozellomycota have the potential to fuel a marine mycoloop. The temporal short and rapid peaking of Rozellomycota *s.l.* may indicate an r-strategists lifestyle, as considered for zoosporic fungal epidemics (Sparrow Jr, 1960; Gleason *et al*., 2012) and further supports the view that the mycoloop is subjected to seasonal changes (Kagami *et al*., 2014).

In this study, we showed that marine unicellular fungi represent an active and dynamic component of coastal communities, whose abundance is comparable to that of filamentous forms. The presence of a small number of taxonomically and ecologically distinct organisms with unique dynamics suggests that a number of niches exist. Such niches incorporate biotic interactions and the cycling of carbon during phytoplankton blooms that can be components of the mycoflux (Grossart *et al*., 2019) and mycoloop (Kagami *et al*., 2014). Furthermore, they are likely linked to primary and secondary consumer food chains and highlight the importance of unicellular fungi in food web structures and carbon transfer.

Experimental procedures

Seawater sampling

Surface seawater samples were taken at Helgoland Roads (54° 11.3′ N, 7° 54.0′ E), at a depth of about 1 m, and processed in the laboratory of the Biologische Anstalt Helgoland (BAH) less than 2 h after sampling. The period between March and May 2017 was covered with 41 samples (Table S3), spanning all stages of the spring phytoplankton bloom, some by daily sampling. At each time point, exactly 1 L of seawater was sequentially filtered through 10 μm, 3 μm and 0.2 μm isopore polycarbonate filters using a vacuum pump (Merck Millipore, Darmstadt, Germany). The filters were placed inside 10 ml cryogenic vials and stored at −80°C.

Physicochemical parameters and phytoplankton data

Environmental parameters were acquired from the BAH as part of the LTER monitoring programme (Wiltshire, 2004). This included data on nutrients (SiO_4, NO_2, NO_3, NH_4 and PO_4), salinity, surface water temperature and cell counts of total phytoplankton and six additional phytoplankton groups, namely Dinophyceae (dinoflagellates), Coccolithophoridae indeterminata (IND), flagellates, Bacillariales (pennate diatoms), Biddulphiales (centric diatoms), Dictyochophyceae (silicoflagellates) and Ciliates (Table S1). The abundance of these phytoplankton groups has also been provided in a graph (Fig. S1).

DNA extraction & PCR amplification

DNA was extracted from 0.2 and 3 μm polycarbonate filters from each time point following a modified SDS-based extraction method after Zhou *et al*. (Zhou *et al*., 1996). The quality of extraction was monitored using agarose gel electrophoresis and a Qubit 2.0 Fluorometer (Invitrogen, Darmstadt, Germany). Extracted genomic material from both fractions for each time point was pooled in equimolar concentrations, resulting in 41 samples. Samples were sent to LGC (Berlin, Germany) for PCR amplification and sequencing using an Illumina MiSeq platform (San Diego, USA) following the manufacturer's instructions. The V8-V9 region of the fungal 18S rRNA gene was amplified using the forward and reverse primer, nu-SSU-1334-5′/nu-SSU-1648-3′ (FF390/FR1, 5′- CGWTAACGAACGAGACCT/3′-ANCCA TTCAATCGGTANT) (Prévost-Bouré *et al*., 2011) described as the best performing 18S rRNA fungi-specific primer pair for marine fungal community surveys (Banos *et al*., 2018); Banos *et al*., 2019). In conjunction with the primers, four blocking oligonucleotides with a 3′-amino linker C6 modification were used to prevent co-amplification of non-fungal eukaryotic groups (Banos *et al*., 2018).

Sequence analysis

Sequence analysis followed the protocol of Banos *et al*. (2020). In short, quality controlled reads were aligned to the non-redundant SILVA SSURef_NR99_132 database (Quast *et al*., 2013), using the SINA aligner v.1.2.11 (Pruesse *et al*., 2012) in ARB (Ludwig *et al*., 2004), with the default settings. Next, sequence reads classified as fungi under a 95% sequence threshold were extracted from the dataset and clustered into OTUs based on 98% sequence similarity using the CD-HIT-EST tool within the CD-HIT programme (Fu *et al*., 2012). Singletons defined to be present only in a single sample with less than five sequence reads were removed from the dataset. The final taxonomic classification was done by placing sequences phylogenetically into the fungal reference tree (Yarza *et al*., 2017) using the Maximum Parsimony algorithm of the ARB programme v6.0.3. The fungal taxonomy used by Yarza *et al*. (2017) was that of the NCBI (National Center for Biotechnology Information) taxonomy database. However, we have adapted it towards the classifications based on Tedersoo *et al*. (2018). Sequences that were positioned on long, erroneous branches were removed from the tree and designated with 'Unclear taxonomic assignment'.

Statistical analysis

All statistical analysis was carried out in R studio version 1.1.463 (R Core Team, 2015) using the *ggplot2* (Wickham, 2016), *phyloseq* (McMurdie and Holmes, 2013),

G*UniFrac* (Chen *et al*., 2012) and *vegan* packages (Oksanen *et al*., 2013). To understand the dynamics in community diversity over the sampling period, the Chao1 and Shannon indices were computed on subsampled datasets. For all other statistical analyses, the total OTU counts were subject to Hellinger transformation (Bhattacharyya, 1943) and the correlating environmental data were standardized using Z-score transformation (Clark-Carter, 2014). Generalized UniFrac distances ($a = 0.05$) (Chen *et al*., 2012) were calculated and the variations in community composition across samples was visualized by Principal coordinates analysis (PCoA). To determine which environmental variables had a significant impact on the variation in community composition and on specific taxa, stepwise model building with permutation tests was performed in 'both' directions with adjusted R^2- and P-value using the 'RDA' and 'ordistep' function in the *vegan* package.

CARD-FISH method development and probe testing

The application of CARD-FISH on marine fungi has only previously been applied in a targeted approach (Hassett *et al*., 2019), whereby a single phylum was at focus. In this study, we aimed to optimize the protocol towards the detection of multiple fungal groups. In total, nine fungal cultures were used, spanning several phyla, for the protocol development. The cultures were first grown on solid agar (Table S4) at 15°C in 9 cm petri dishes in the dark and subsequently transferred to liquid media. Within 7–14 days, they grew to dense cultures, which were harvested on 3 μm pore-size polycarbonate filters.

The established CARD-FISH protocol for marine bacteria (Pernthaler and Amann, 2004; Thiele *et al*., 2011) was used as a guideline. For all protocol testing steps, the eukaryotic probe EUK516 (5′-ACC AGA CTT GCC CTC C-3′) (Amann *et al*., 1990) was used, after ensuring its match to the 18S rRNA of the cultures using the fungal reference dataset (Yarza *et al*., 2017) within the ARB programme. The primary focus of optimization was the permeabilization step, due to the different cell wall structure of fungi. In order to permeabilise the cell wall without causing a loss of integrity, enzymes were tested in varying concentrations and under a range of incubation conditions. The chosen enzymes were chitinase (Sigma Aldrich, Darmstadt, Germany) and Glucanex (Sigma Aldrich). Glucanex is an enzyme cocktail isolated from *Trichoderma harzianum* that contains β-glucanase, cellulase, protease and chitinase (for the detailed parameters tested, see Table S5). The CARD-FISH optimization was considered successful once >75% of the cells or filaments present in the different cultures were detected. The most effective permeabilization protocol was an incubation for 1 h at 30°C in a permeabilization buffer consisting of 1x PBS (0.137 M NaCl, 0.0027 M KCl, 0.01 M Na_2HPO_4, 0.0018 M KH_2PO_4, pH 7.4), 1% SDS, pH 6.5, 1 mg ml^{-1} chitinase and 6 mg ml^{-1} Glucanex. The final protocol includes seven steps from sample preparation to the final counter-staining (Table S6).

Probe design

Seven 18S rRNA-targeted oligonucleotide probes were designed, using the in-built 'probe design' function in ARB. Probes were purchased from 'biomers.net' (Ulm, Germany) with a horseradish peroxidase ligated to the 5′ end (Table 3). A fungal reference database (Yarza *et al*., 2017) holding 9329 nearly full-length representative 18S rRNA gene sequences was complemented with the partial 18S rRNA sequence of non-singleton OTUs from this study. Sequences were aligned using the RAxML programme (Stamatakis, 2014), integrated in ARB. Probe specificity was assessed using this database and the SILVA SSU Ref NR99 database (release 132). Where necessary, competitor probes were designed, to block known single mismatch non-target sequences, and helper probes (Fuchs *et al*., 2000) were designed to improve binding efficiency where necessary. Thermodynamics and kinetics of probe accessibility and binding were further checked with mathFISH (Yilmaz *et al*., 2011). Probes were tested on pure cultures, where available, or on environmental samples, applying the protocol outlined above and testing a range of formamide concentrations (0% – 40%) (Table 3). The optimal formamide concentration was determined as the highest concentration possible before signal probe signal intensity reduced. Probes were classified as successful when >75% of the filaments present showed a hybridized signal (Fig. S7). Probe testing on environmental samples was performed by hybridizing fractions of the same sample with the designed probe, the EUK516 and EUBI-III probe (as a negative control). Probes were deemed successful when the hybridized signal from the designed probe coincided with the same cell morphologies that were identified with the EUK516 probe but not with the EUBI-III probe.

CARD-FISH environmental testing and application

Initial tests on three environmental samples that covered the pre-, mid- and post- bloom stage were carried out to ensure the protocol was effective on marine fungi and did not result in any non-specific hybridization. These tests were performed with probes FAsc_1094, FBas_757, EUK516, the general bacterial probe mix EUBI-III (I: GCTGCCTCCCGTAGGAGT, II: GCAGCCACCCGTAGGTGT, III: GCTGCCACCCGTAGG TGT) (Amann *et al*., 1990; Daims *et al*., 1999) and the negative control NONEUB (ACTCCTACGGGAGGCAGC) (Wallner *et al*., 1993), using the newly optimized

Table 3. CARD-FISH oligonucleotide probes designed for fungal taxa along with their respective competitor and helper probes.

Name	Sequence (5′-3′)	Target group (coverage %)	Formamide (%)	Competitor name	Competitor sequence
FAsc_1094	GGUCUCGUUCGUUAUCGCAA	Ascomycota	20	FAsc_1094_C3	GGTCTCGTTCGTTATCGGAA
				FAsc_1094_C6	GGTCTCGTTCGTTAACGCAA
				FAsc_1094_C6G	GGTCTCGTTCGTTACCGCAA
FBas_757	CCCUAACCUUCGUUCUUG	Basidiomycota	20		
FPucc_311	UUUCUCAGGCCCUCUCUCC	Pucciniomycotina	20	FPucc_311_C7	TTTCTCAGGCCCCCTCTCC
				FPucc_311C7-18	TCTCTCAGGCCCCCTCTCC
				FPucc_311_C7U-18	TCTCTCAGGCCCACTCTCC
				Helper name	**Helper sequence**
FLKM2_1129	GCGGAACCCGAAAAUUCAC	OTU571, LKM11 Clade 2	10	FLKM2_H	ACUUUUAUUAAGCAGUUUA
FLKM2_1162	GCCAACCAAUAAGCCUGG			FLKM2_Hb	UUAGUCCCUCUAAGAAGACGC
				FLKM1_Hc	AGACCUGUUAUUGCCUCAAACU
FLKM3_1115	UCGUAGCAUGACAGGUAG	OTU209, LKM11 Clade 3	5	FLKM3_H	GCCUGCCGAUUCACACAUCAACAG
FLKM3_1145	GUCAGUCCCUCAUAGAAC			FLKM3_H	UGGGGUUACCAGUAGGAAGUUU

permeabilization protocol for fungi and the original permeabilization protocol for bacteria (Pernthaler and Amann, 2004). Fluorescence signals obtained with EUK516 and fungi-specific probes were distinctly different to the signals for the EUBI-III and the negative control. Following successful testing, the probes were applied to 0.2 μm and 3 μm filters from 26 time points during the sampling period. Additionally, several 10 μm filters were screened for potentially attached parasitic fungi to phytoplankton cells. Samples were viewed using a Zeiss Axio imager D2 microscope (Zeiss, Oberkochen, Germany) at 100x magnification and quantified according to Thiele *et al*. (2011). To provide further validation that probes were binding to fungal cells, we applied a combination of the FBas_757 probe with CalcoFluor White (Sigma-Aldrich) staining and analysed the result under a confocal laser scanning microscope (Zeiss ELYRA LSM780). A successful reaction was determined with ovoid cell shapes containing the probe signal in the interior of the cell and a CalcoFluor White signal on the perimeter of the cell (Fig. S6). Statistical analysis of absolute cell counts and measured environmental parameters was then performed as outlined in the respective section. Additionally, the biovolume of the yeast (−like) cells was converted to biomass by taking the average value of all observed cells and applying the yeast-specific conversion factor proposed by van Veen and Paul (1979) of 1 μm^3 = 0.8 pg C.

Acknowledgements

The authors are grateful to Karen Wiltshire and the staff of the Biological Station Helgoland of the Alfred Wegener Institute for Polar and Marine Research who provided the data on abiotic parameters and the phytoplankton counts and continue to perform these tasks as part of the LTER monitoring series. The authors would also like to thank the technicians of the Department of Molecular Ecology, Max Planck Institute for Marine Microbiology, for their technical support throughout this study. This study was funded by the Max Planck Society.

Data availability

Sequencing data used in this study has been submitted to ENA under the accession number PRJEB36396. The ARB database file, containing the phylogenetic tree, and the annotated OTU table have been supplied as supplementary files (Appendices S1 and S2 respectively).

References

Amann, R.I., Binder, B.J., Olson, R.J., Chisholm, S.W., Devereux, R., Stahl, D.A. (1990). Combination of 16S rRNA-targeted oligonucleotide probes with flow cytometry for analyzing mixed microbial populations. *Applied and Environmental Microbiology*, **56**: 1919–1925. http://dx.doi.org/10.1128/aem.56.6.1919-1925.1990.

Banos, S., Gysi, D.M., Richter-Heitmann, T., Glöckner, F.O., and Boersma, M. (2020) Seasonal dynamics of pelagic mycoplanktonic communities: interplay of taxon abundance, temporal occurrence, and biotic interactions. *Front Microbiol* **11**: Artnr1305. https://doi.org/10.3389/fmicb.2020.01305.

Banos, S., Lentendu, G. Kopf, A. Wubet, T., Glöckner, F.O., and Reich, M. (2019) Correction to: A comprehensive fungi-specific 18S rRNA gene sequence primer toolkit suited for diverse research issues and sequencing platforms. *BMC Microbiol* **19**: 249. https://doi.org/10.1186/s12866-019-1628-y.

Banos, S., Lentendu, G., Kopf, A., Wubet, T., Glöckner, F.O., and Reich, M. (2018) A comprehensive fungi-specific 18S rRNA gene sequence primer toolkit suited for diverse research issues and sequencing platforms. *BMC Microbiol* **18**: 190. https://doi.org/10.1186/s12866-018-1331-4.

Bhattacharyya, A. (1943) On a measure of divergence between two statistical populations defined by their probability distributions. *Bull Calcutta Math Soc* **35**: 99–109. https://www.jstor.org/stable/25047882?seq=1#metadata_info_tab_contents.

Buchan, A., LeCleir, G.R., Gulvik, C.A., and González, J.M. (2014) Master recyclers: features and functions of bacteria associated with phytoplankton blooms. *Nat Rev Microbiol* **12**: 686–698. https://doi.org/10.1038/nrmicro3326.

Chafee, M., Fernàndez-Guerra, A., Buttigieg, P.L., Gerdts, G., Eren, A.M., Teeling, H., and Amann, R.I. (2018) Recurrent patterns of microdiversity in a temperate coastal marine environment. *ISME J* **12**: 237–252. https://doi.org/10.1038/ismej.2017.165.

Chen, J., Bittinger, K., Charlson, E.S., Hoffmann, C., Lewis, J., Wu, G.D., *et al*. (2012) Associating microbiome composition with environmental covariates using generalized UniFrac distances. *Bioinformatics* **28**: 2106–2113. https://doi.org/10.1093/bioinformatics/bts342.

Clark-Carter, D. (2014) z scores. In Balakrishnan, N., Colton, T., Everitt, B., Piegorsch, W., Ruggeri, F., and Teugels, J.L. (eds.). *Wiley StatsRef: Statistics Reference Online*, New York, NY: American Cancer Society. https://doi.org/10.1002/9781118445112.stat06236.

Comeau, A.M., Vincent, W.F., Bernier, L., and Lovejoy, C. (2016) Novel chytrid lineages dominate fungal sequences in diverse marine and freshwater habitats. *Sci Rep* **6**: 30120. https://doi.org/10.1038/srep30120.

Cunliffe, M., Hollingsworth, A., Bain, C., Sharma, V., and Taylor, J.D. (2017) Algal polysaccharide utilisation by saprotrophic planktonic marine fungi. *Fungal Ecol* **30**: 135–138. https://doi.org/10.1016/j.funeco.2017.08.009.

Daims, H., Brühl, A., Amann, R., Schleifer, K.-H., and Wagner, M. (1999) The domain-specific probe EUB338 is insufficient for the detection of all bacteria: development and evaluation of a more comprehensive probe set. *Syst Appl Microbiol* **22**: 434–444. https://doi.org/10.1016/S0723-2020(99)80053-8.

de Vargas, C., Audic, S., Henry, N., Decelle, J., Mahé, F., Logares, R., *et al*. (2015) Eukaryotic plankton diversity in the sunlit ocean. *Science* **348**: 1261605. https://doi.org/10.1126/science.1261605.

Duan, Y., Xie, N., Song, Z., Ward, C.S., Yung, C.-M., Hunt, D.E., *et al*. (2018) High-resolution time-series reveals seasonal patterns of planktonic fungi at a temperate coastal ocean site (Beaufort, North Carolina, USA). *Appl Environ Microbiol* **84**: e00967–e00918. https://doi.org/10.1128/AEM.00967-18.

Falkowski, P.G., Barber, R.T., and Smetacek, V. (1998) Biogeochemical controls and feedbacks on ocean primary production. *Science* **281**: 200–206. https://doi.org/10.1126/science.281.5374.200.

Field, C.B., Behrenfeld, M.J., Randerson, J.T., and Falkowski, P. (1998) Primary production of the biosphere: integrating terrestrial and oceanic components. *Science* **281**: 237–240. https://doi.org/10.1126/science.281.5374.237.

Francis, M.M., Webb, V., and Zuccarello, G.C. (2016) Marine yeast biodiversity on seaweeds in New Zealand waters. *N Z J Bot* **54**: 30–47. https://doi.org/10.1080/0028825X.2015.1103274.

Frenken, T., Wierenga, J., Donk, E., Declerck, S.A.J., Senerpont Domis, L.N., Rohrlack, T., and Van de Waal, D.B. (2018) Fungal parasites of a toxic inedible cyanobacterium provide food to zooplankton. *Limnol Oceanogr* **63**: 2384–2393. https://doi.org/10.1002/lno.10945.

Fu, L., Niu, B., Zhu, Z., Wu, S., and Li, W. (2012) CD-HIT: accelerated for clustering the next-generation sequencing data. *Bioinformatics* **28**: 3150–3152. https://doi.org/10.1093/bioinformatics/bts565.

Fuchs, B.M., Glöckner, F.O., Wulf, J., and Amann, R. (2000) Unlabeled helper oligonucleotides increase the in situ accessibility to 16S rRNA of fluorescently labeled oligonucleotide probes. *Appl Environ Microbiol* **66**: 3603–3607. https://doi.org/10.1128/aem.66.8.3603-3607.2000.

Gancedo, J.M. (1986) Carbohydrate metabolism in yeast. In Morgan, M.J., (ed.), *Carbohydrate Metabolism in Cultured Cells*. Boston: Springer. https://doi.org/10.1007/978-1-4684-7679-8_8.

Gleason, F.H., Carney, L.T., Lilje, O., and Glockling, S.L. (2012) Ecological potentials of species of Rozella (Cryptomycota). *Fungal Ecol* **5**: 651–656. https://doi.org/10.1016/j.funeco.2012.05.003.

Grossart, H.-P., Van den Wyngaert, S., Kagami, M., Wurzbacher, C., Cunliffe, M., and Rojas-Jimenez, K. (2019) Fungi in aquatic ecosystems. *Nat Rev Microbiol* **17**: 339–354. https://doi.org/10.1038/s41579-019-0175-8.

Gutiérrez, M., Pantoja, S., Tejos, E., and Quinones, R. (2010) Role of fungi in processing marine organic matter in the upwelling ecosystem off Chile. *Mar Biol* **158**: 205–219. https://doi.org/10.1007/s00227-010-1552-z.

Gutiérrez, M.H., Jara, A.M., and Pantoja, S. (2016) Fungal parasites infect marine diatoms in the upwelling ecosystem of the Humboldt current system off Central Chile: fungal parasites on marine diatoms in upwelling ecosystems. *Environ Microbiol* **18**: 1646–1653. https://doi.org/10.1111/1462-2920.13257.

Hagler, A.N. (2006) Yeasts as indicators of environmental quality. In Péter, G., and Rosa, C. (eds). *Biodiversity and Ecophysiology of Yeasts, the Yeast Handbook*. Berlin Heidelberg: Springer, pp. 515–532. https://doi.org/10.1007/3-540-30985-3_21.

Hagler, A.N., and Mendonça-Hagler, L.C. (1981) Yeasts from marine and estuarine waters with different levels of pollution in the state of Rio de Janeiro. *Brazil Appl Environ Microbiol* **41**: 173–178. https://doi.org/10.1128/aem.41.1.173-178.1981.

Hassett, B.T., Borrego, E.J., Vonnahme, T.R., Rämä, T., Kolomiets, M.V., and Gradinger, R. (2019) Arctic marine fungi: biomass, functional genes, and putative ecological roles. *ISME J* **13**: 1484–1496. https://doi.org/10.1038/s41396-019-0368-1.

Hassett, B.T., Ducluzeau, A.-L.L., Collins, R.E., and Gradinger, R. (2016) Spatial distribution of aquatic marine fungi across the western Arctic and sub-arctic. *Environ Microbiol* **19**: 475–484. https://doi.org/10.1111/1462-2920.13371.

Hassett, B.T., and Gradinger, R. (2016) Chytrids dominate arctic marine fungal communities. *Environ Microbiol* **18**: 2001–2009. https://doi.org/10.1111/1462-2920.13216.

Heitman, J., Howlett, B.J., Crous, P.W., Stukenbrock, E.H., James, T.Y., Gow, N.A.R. (2017). The Fungal Kingdom, American Society of Microbiology. https://doi.org/10.1128/9781555819583.

Hickel, W., Berg, J., and Treutner, K. (1992) Variability in phytoplankton biomass in the German bight near Helgoland, 1980-1990. *ICES Mar Sci Symp* **195**: 249–259.

James, T.Y., and Berbee, M.L. (2011) No jacket required – new fungal lineage defies dress code. *Bioessays* **34**: 94–102. https://doi.org/10.1002/bies.201100110.

James, T.Y., Pelin, A., Bonen, L., Ahrendt, S., Sain, D., Corradi, N., and Stajich, J. (2013) Shared signatures of parasitism and phylogenomics unite Cryptomycota and microsporidia - ScienceDirect. *Curr Biol* **23**: 1548–1553. https://doi.org/10.1016/j.cub.2013.06.057.

Jeffries, T.C., Curlevski, N.J., Brown, M.V., Harrison, D.P., Doblin, M.A., Petrou, K., *et al*. (2016) Partitioning of fungal assemblages across different marine habitats. *Environ Microbiol Rep* **8**: 235–238. https://doi.org/10.1111/1758-2229.12373.

Jobard, M., Rasconi, S., and Sime-Ngando, T. (2010) Fluorescence in situ hybridization of uncultured zoosporic fungi: testing with clone-FISH and application to freshwater samples using CARD-FISH. *J Microbiol Methods* **83**: 236–243. https://doi.org/10.1016/j.mimet.2010.09.006.

Jones, M.D.M., Forn, I., Gadelha, C., Egan, M.J., Bass, D., Massana, R., and Richards, T.A. (2011) Discovery of novel intermediate forms redefines the fungal tree of life. *Nature* **474**: 200. https://doi.org/10.1038/nature09984.

Jørgensen, N.O.G., and Stepanauskas, R. (2009) Biomass of pelagic fungi in Baltic rivers. *Hydrobiologia* **623**: 105–112. https://doi.org/10.1007/s10750-008-9651-2.

Kagami, M., de Bruin, A., Ibelings, B.W., and Van Donk, E. (2007) Parasitic chytrids: their effects on phytoplankton communities and food-web dynamics. *Hydrobiologia* **578**: 113–129. https://doi.org/10.1007/s10750-006-0438-z.

Kagami, M., Miki, T., and Takimoto, G. (2014) Mycoloop: chytrids in aquatic food webs. *Front Microbiol* **5**: 166. https://doi.org/10.3389/fmicb.2014.00166.

Kurtzman, C.P., Fell, J.W., and Boekhout, T. (2011) *The Yeasts: A Taxonomic Study*, 5th ed. London, UK: Elsevier. https://www.elsevier.com/books/the-yeasts/kurtzman/978-0-444-52149-1.

Kutty, S.N., and Philip, R. (2008) Marine yeasts-a review. *Yeast Chichester Engl* **25**: 465–483. https://doi.org/10.1002/yea.1599.

Lara, E., Moreira, D., and López-García, P. (2010) The environmental clade LKM11 and Rozella form the deepest branching clade of fungi. *Protist* **161**: 116–121. https://doi.org/10.1016/j.protis.2009.06.005.

Letcher, P.M., and Powell, M.J. (2018) A taxonomic summary and revision of Rozella (Cryptomycota). *IMA Fungus* **9**: 383–399. https://doi.org/10.5598/imafungus.2018.09.02.09.

Livermore, J.A., and Mattes, T.E. (2013) Phylogenetic detection of novel Cryptomycota in an Iowa (United States) aquifer and from previously collected marine and freshwater targeted high-throughput sequencing sets. *Environ Microbiol* **15**: 2333–2341. https://doi.org/10.1111/1462-2920.12106.

Loque, C.P., Medeiros, A.O., Pellizzari, F.M., Oliveira, E.C., Rosa, C.A., and Rosa, L.H. (2010) Fungal community associated with marine macroalgae from Antarctica. *Polar Biol* **33**: 641–648. https://doi.org/10.1007/s00300-009-0740-0.

Ludwig, W., Strunk, O., Westram, R., Richter, L., Meier, H., Yadhukumar A., *et al*. (2004) ARB: a software environment for sequence data. *Nucleic Acids Res* **32**: 1363–1371. https://doi.org/10.1093/nar/gkh293.

MacGillivray, A.R., and Shiaris, M.P. (1993) Biotransformation of polycyclic aromatic hydrocarbons by yeasts isolated from coastal sediments. *Appl Environ Microbiol* **59**: 1613–1618. https://doi.org/10.1128/aem.59.5.1613-1618.1993.

McMurdie, P.J., and Holmes, S. (2013) Phyloseq: an R package for reproducible interactive analysis and graphics of microbiome census data. *PLoS One* **8**: e61217. https://doi.org/10.1371/journal.pone.0061217.

Meyers, S.P., Ahearn, D.G., Gunkel, W., and Roth, F.J. (1967) Yeasts from the North Sea. *Mar Biol* **1**: 118–123. https://doi.org/10.1007/BF00386516.

Mitchison-Field, L.M.Y., Vargas-Muñiz, J.M., Stormo, B.M., Vogt, E.J.D., Dierdonck, S.V., Ehrlich, C., *et al*. (2019) Unconventional cell division cycles from marine-derived yeasts. *Current Biology* **29**: 1–18. https://doi.org/10.1101/657254.

Nikolcheva, L.G., Cockshutt, A.M., and Bärlocher, F. (2003) Determining diversity of freshwater fungi on decaying leaves: comparison of traditional and molecular approaches. *Appl Environ Microbiol* **69**: 2548–2554. https://doi.org/10.1128/AEM.69.5.2548-2554.2003.

Oksanen, J., Blanchet, F.G., Kindt, R., Legendre, P., Minchin, P., O'Hara, R., *et al*. (2013). Vegan: Community Ecology Package. R Package Version. 2.0–10. CRAN. Retrieved from https://github.com/vegandevs/vegan

Pernthaler, A., and Amann, R. (2004) Simultaneous fluorescence in situ hybridization of mRNA and rRNA in environmental bacteria. *Appl Environ Microbiol* **70**: 5426–5433. https://doi.org/10.1128/AEM.70.9.5426-5433.2004.

Pernthaler, A., Pernthaler, J., and Amann, R. (2002) Fluorescence in situ hybridization and catalyzed reporter deposition for the identification of marine bacteria. *Appl Environ Microbiol* **68**: 3094–3101. https://doi.org/10.1128/aem.68.6.3094-3101.2002.

Picard, K.T. (2017) Coastal marine habitats harbor novel early-diverging fungal diversity. *Fungal Ecol* **25**: 1–13. https://doi.org/10.1016/j.funeco.2016.10.006.

Prévost-Bouré, N.C., Christen, R., Dequiedt, S., Mougel, C., Lelièvre, M., Jolivet, C., *et al*. (2011) Validation and application of a PCR primer set to quantify fungal communities in the

soil environment by real-time quantitative PCR. *PLoS One* **6**: e24166. https://doi.org/10.1371/journal.pone.0024166.

Pruesse, E., Peplies, J., and Glöckner, F.O. (2012) SINA: accurate high-throughput multiple sequence alignment of ribosomal RNA genes. *Bioinformatics* **28**: 1823–1829. https://doi.org/10.1093/bioinformatics/bts252.

Quast, C., Pruesse, E., Yilmaz, P., Gerken, J., Schweer, T., Yarza, P., *et al*. (2013) The SILVA ribosomal RNA gene database project: improved data processing and web-based tools. *Nucleic Acids Res* **41**: D590–D596. https://doi.org/10.1093/nar/gks1219.

R Core Team. (2015) *A Language and Environment for Statistical Computing*. Vienna, Austria: R Foundation for statistical computing. [WWW document]. https://www.r-project.org/foundation/.

Rasconi, S., Jobard, M., Jouve, L., and Sime-Ngando, T. (2009) Use of Calcofluor White for detection, identification, and quantification of Phytoplanktonic fungal parasites. *Appl Environ Microbiol* **75**: 2545–2553. https://doi.org/10.1128/AEM.02211-08.

Ravelet, C., Grosset, C., Krivobok, S., Montuelle, B., and Alary, J. (2001) Pyrene degradation by two fungi in a freshwater sediment and evaluation of fungal biomass by ergosterol content. *Appl Microbiol Biotechnol* **56**: 803–808. https://doi.org/10.1007/s002530100689.

Rojas-Jimenez, K., Rieck, A., Wurzbacher, C., Jürgens, K., Labrenz, M., and Grossart, H.P. (2019) A salinity threshold separating fungal communities in the Baltic Sea. *Front Microbiol* **10**: Artnr680. https://doi.org/10.3389/fmicb.2019.00680.

Rojas-Jimenez, K., Wurzbacher, C., Bourne, E.C., Chiuchiolo, A., Priscu, J.C., and Grossart, H.P. (2017) Early diverging lineages within Cryptomycota and Chytridiomycota dominate the fungal communities in ice-covered lakes of the McMurdo Dry Valleys. *Antarctica Sci Rep* **7**: 1–11. https://doi.org/10.1038/s41598-017-15598-w.

Rosa, C.A., and Péter, G. (2006) *The Yeast Handbook: Biodiversity and Ecophysiology of Yeasts*. Berlin Heidelberg: Springer. https://doi.org/10.1007/3-540-30985-3_21.

Scholz, B., Guillou, L., Marano, A.V., Neuhauser, S., Sullivan, B.K., Karsten, U., *et al*. (2016) Zoosporic parasites infecting marine diatoms — a black box that needs to be opened. *Fungal Ecol* **19**: 59–76. https://doi.org/10.1016/j.funeco.2015.09.002.

Sime-Ngando, T. (2012) Phytoplankton Chytridiomycosis: fungal parasites of phytoplankton and their imprints on the food web dynamics. *Front Microbiol* **3**: 361. https://doi.org/10.3389/fmicb.2012.00361.

Slater, M.L., Sharrow, S.O., and Gart, J.J. (1977) Cell cycle of Saccharomycescerevisiae in populations growing at different rates. *Proc Natl Acad Sci* **74**: 3850–3854. https://doi.org/10.1073/pnas.74.9.3850.

Sparrow, F.K., Jr. (1960) *Aquatic Phycomycetes*, 2nd ed. Ann Arbor, MI, USA: The University of Michigan Press. https://doi.org/10.5962/bhl.title.5685.

Stamatakis, A. (2014) RAxML version 8: a tool for phylogenetic analysis and post-analysis of large phylogenies. *Bioinformatics* **30**: 1312–1313. https://doi.org/10.1093/bioinformatics/btu033.

Suksomjit, M., Nagao, S., Ichimi, K., Yamada, T., and Tada, K. (2009) Variation of dissolved organic matter and fluorescence characteristics before, during and after phytoplankton bloom. *J Oceanogr* **65**: 835–846. https://doi.org/10.1007/s10872-009-0069-x.

Taib, N., Mangot, J.-F., Domaizon, I., Bronner, G., and Debroas, D. (2013) Phylogenetic affiliation of SSU rRNA genes generated by massively parallel sequencing: new insights into the freshwater Protist diversity. *PLoS One* **8**: e58950. https://doi.org/10.1371/journal.pone.0058950.

Taylor, J.D., and Cunliffe, M. (2016) Multi-year assessment of coastal planktonic fungi reveals environmental drivers of diversity and abundance. *ISME J* **10**: 2118–2128. https://doi.org/10.1038/ismej.2016.24.

Tedersoo, L., Sánchez-Ramírez, S., Kõljalg, U., Bahram, M., Döring, M., Schigel, D., *et al*. (2018) High-level classification of the fungi and a tool for evolutionary ecological analyses. *Fungal Divers* **90**: 135–159. https://doi.org/10.1007/s13225-018-0401-0.

Teeling, H., Fuchs, B.M., Becher, D., Klockow, C., Gardebrecht, A., Bennke, C.M., *et al*. (2012) Substrate-controlled succession of marine Bacterioplankton populations induced by a phytoplankton bloom. *Science* **336**: 608–611. https://doi.org/10.1126/science.1218344.

Teeling, H., Fuchs, B.M., Bennke, C.M., Krüger, K., Chafee, M., Kappelmann, L., *et al*. (2016) Recurring patterns in bacterioplankton dynamics during coastal spring algae blooms. *eLife* **5**: e11888. https://doi.org/10.7554/eLife.11888.

Thiele, S., Fuchs, B.M., and Amann, R.I. (2011) Identification of microorganisms using the ribosomal RNA approach and fluorescence in situ hybridization. In *Treatise on Water Science*, Amsterdam: Elsevier, pp. 171–189. https://doi.org/10.1016/b978-0-444-53199-5.00056-7.

Thornton, D.C.O. (2014) Dissolved organic matter (DOM) release by phytoplankton in the contemporary and future ocean. *Eur J Phycol* **49**: 20–46. https://doi.org/10.1080/09670262.2013.875596.

Tian, T., Merico, A., Su, J., Staneva, J., Wiltshire, K., and Wirtz, K. (2009) Importance of resuspended sediment dynamics for the phytoplankton spring bloom in a coastal marine ecosystem. *J Sea Res* **62**: 214–228. https://doi.org/10.1016/j.seares.2009.04.001.

Tisthammer, K.H., Cobian, G.M., and Amend, A.S. (2016) Global biogeography of marine fungi is shaped by the environment. *Aquat Fungi* **19**: 39–46. https://doi.org/10.1016/j.funeco.2015.09.003.

Torruella, G., Grau-Bové, X., Moreira, D., Karpov, S.A., Burns, J.A., Sebé-Pedrós, A., *et al*. (2018) Global transcriptome analysis of the aphelid Paraphelidium tribonemae supports the phagotrophic origin of fungi. *Commun Biol* **1**: 1–11. https://doi.org/10.1038/s42003-018-0235-z.

van den Wollenberg, A.L. (1977) Redundancy analysis an alternative for canonical correlation analysis. *Psychometrika* **42**: 207–219. https://doi.org/10.1007/BF02294050.

van Veen, J.A., and Paul, E.A. (1979) Conversion of biovolume measurements of soil organisms, grown under various moisture tensions, to biomass and their nutrient content. *Appl Environ Microbiol* **37**: 686–692. https://doi.org/10.1128/aem.37.4.686-692.1979.

Voigt, K., Marano, A.V., and Gleason, F.H. (2013) 9 Ecological and economical importance of parasitic Zoosporic true

fungi. In Kempken, F. (ed). *Agricultural Applications*. Berlin, Germany: Springer, pp. 243–270. https://doi.org/10.1007/978-3-642-36821-9_9.

Wagner, M., and Haider, S. (2012) New trends in fluorescence in situ hybridization for identification and functional analyses of microbes. *Curr Opin Biotechnol* **23**: 96–102. https://doi.org/10.1016/j.copbio.2011.10.010.

Wallner, G., Amann, R., and Beisker, W. (1993) Optimizing fluorescent in situ hybridization with rRNA-targeted oligonucleotide probes for flow cytometric identification of microorganisms. *Cytometry* **14**: 136–143. https://doi.org/10.1002/cyto.990140205.

Wang, Q.-M., Yurkov, A.M., Göker, M., Lumbsch, H.T., Leavitt, S.D., Groenewald, M., *et al*. (2015) Phylogenetic classification of yeasts and related taxa within Pucciniomycotina. *Stud Mycol* **81**: 149–189. https://doi.org/10.1016/j.simyco.2015.12.002.

Wang, X., Singh, P., Gao, Z., Zhang, X., Johnson, Z.I., and Wang, G. (2014) Distribution and diversity of planktonic fungi in the West Pacific warm Pool. *PLoS One* **9**: e101523. https://doi.org/10.1371/journal.pone.0101523.

Weete, J.D., Abril, M., and Blackwell, M. (2010) Phylogenetic distribution of fungal sterols. *PLoS One* **5**: e10899. https://doi.org/10.1371/journal.pone.0010899.

Wickham, H. (2016) *ggplot2: Elegant Graphics for Data Analysis*. New York: Springer. https://doi.org/10.1007/978-0-387-98141-3.

Wijayawardene, N.N., Hyde, K.D., Al-Ani, L.K.T., Tedersoo, L., Haelewaters, D., Rajeshkumar, K.C., *et al*. (2020) Outline of fungi and fungus-like taxa. *Mycosphere* **11**: 1060–1456. https://doi.org/10.5943/mycosphere/11/1/8.

Wiltshire, K.H. (2004) Editorial on Helgoland roads time series. *Helgol Mar Res* **58**: 221–222. https://doi.org/10.1007/s10152-004-0198-y.

Wiltshire, K.H., Kraberg, A., Bartsch, I., Boersma, M., Franke, H.-D., Freund, J., *et al*. (2010) Helgoland roads, North Sea: 45 years of change. *Estuaries Coast* **33**: 295–310. https://doi.org/10.1007/s12237-009-9228-y.

Wurzbacher, C., Grimmett, I.J., and Bärlocher, F. (2015) Metabarcoding-based fungal diversity on coarse and fine particulate organic matter in a first-order stream in Nova Scotia, Canada. *F1000Research* **4**: 1378. https://doi.org/10.12688/f1000research.7359.2.

Wurzbacher, C., Rösel, S., Rychła, A., and Grossart, H.P. (2014) Importance of saprotrophic freshwater fungi for pollen degradation. *PLoS One* **9**: e94643. https://doi.org/10.1371/journal.pone.0094643.

Yarza, P., Yilmaz, P., Panzer, K., Glöckner, F.O., and Reich, M. (2017) A phylogenetic framework for the kingdom fungi based on 18S rRNA gene sequences. *Mar Genomics* **36**: 33–39. https://doi.org/10.1016/j.margen.2017.05.009.

Yilmaz, L.S., Parnerkar, S., and Noguera, D.R. (2011) mathFISH, a web tool that uses thermodynamics-based mathematical models for in silico evaluation of oligonucleotide probes for fluorescence in situ hybridization. *Appl Environ Microbiol* **77**: 1118–1122. https://doi.org/10.1128/AEM.01733-10.

Zhang, H., Jia, J., Chen, S., Huang, T., Wang, Y., Zhao, Z., *et al*. (2018) Dynamics of bacterial and fungal communities during the outbreak and decline of an algal bloom in a drinking water reservoir. *Int J Environ Res Public Health* **15**: 361. https://doi.org/10.3390/ijerph15020361.

Zhang, T., Fei Wang, N., Qin Zhang, Y., Yu Liu, H., and Yan Yu, L. (2015) Diversity and distribution of fungal communities in the marine sediments of Kongsfjorden, Svalbard (High Arctic). *Sci Rep* **5**: 14524. https://doi.org/10.1038/srep14524.

Zhou, J., Bruns, M.A., and Tiedje, J.M. (1996) DNA recovery from soils of diverse composition. *Appl Environ Microbiol* **62**: 316–322. https://doi.org/10.1128/aem.62.2.316-322.1996.

Supporting Information

Additional Supporting Information may be found in the online version of this article at the publisher's web-site:

Table S1 Contextual data used in this study including abiotic parameters and phytoplankton taxa counts obtained from microscopy. All data in this table were provided by the Biologische Anstalt Helgoland station as part of the long-term ecological research series.

Table S2. Cell counts (cells L^{-1}) of the dominant fungal groups obtained using the designed 18S rRNA gene oligonucleotide probes. There were no visible signals for the probes targeting the Ascomycota, Basidiomycota and Pucciniomycota on the 0.2–3 μm fraction and thus only the 3–10 μm fraction values are shown.

Table S3. Sampling time points used in this study.

Table S4. Fungal cultures used in the development of the CARD-FISH protocol with their respective classification and growth media.

Table S5. Parameters tested for permeabilization of fixed fungal cultures on 3 μm pore-size filters. Every possible combination of the parameters outlined below was tested.

Table S6. Protocol of the optimized fungal CARD-FISH procedure. The hybridization, washing and amplification buffer recipes were obtained from Thiele et al. (20112011).

Fig. S1. Microscopy cell counts of the major phytoplankton groups at Helgoland Roads during the sampling period.

Fig. S2. Sketch of a reduced phylogenetic tree of the fungal kingdom with the novel environmental clades identified. Original fungal 18S rRNA gene sequence reference tree derived from Yarza *et al*. (20112017). New clades were designated where clusters of OTUs formed sister branches to previously described lineages; these clusters are represented in green. This tree represents a reduced version of the complete phylogenetic tree, where only the most prominent taxa and those containing novel environmental clades are included, for ease of visualization.

Fig. S3. Alpha richness and diversity of mycoplankton communities at Helgoland Roads over the sampling period.

Fig. S4. Relative read abundance of the most prominent taxa (>2% abundance threshold). A. phylum level classification and B. class or clade level classification. Above the relative read abundance bar chart is the chlorophyll *a* values obtained on the same sampling days and measured using a BBE Fluorometer.

Fig. S5. Redundancy analysis ordination representing the influence of measured parameters on individual OTUs.

Fig. S6. Confocal laser scanning microscopy images of fungal cells. Blue = staining with CalcoFluor White and Red = staining with the Basidiomycota specific FBas_757 probe. The images from the top left to the bottom right represent focal planes in the z direction (moving through the cell from the bottom to the top).

Fig. S7. Epifluorescence microscopy image of hybridized fungal filaments from a pure culture, using a probe designed for the Basidiomycota phylum (FBas_757). Green = probe signal, Blue = DAPI stain.

Appendix S1. ARB database file containing the fungal phylogenetic tree derived from Yarza *et al*. (2017) with the addition of non-singleton OTUs from this study.

Appendix S2. Annotated OTU table containing all non-singleton OTUs, their taxonomic affiliation and total read number for each sampling time point.